A&A 367, 347–354 (2001)
DOI: 10.1051/0004-6361:20000341


Astronomy & Astrophysics

# UV photodestruction of CH bonds and the evolution of the 3.4 $\mu$m feature carrier

## I. The case of aliphatic and aromatic molecular species

G. M. Muñoz Caro[1], R. Ruiterkamp[1], W. A. Schutte[1], J. M. Greenberg[1], and V. Mennella[2]

[1] Raymond and Beverly Sackler Laboratory for Astrophysics at Leiden Observatory, 2300 RA Leiden, The Netherlands
[2] Osservatorio Astronomico di Capodimonte, via Moiariello 16, 80131 Napoli, Italy

Received 26 June 2000 / Accepted 28 November 2000

**Abstract.** Experiments simulating the processing of various hydrocarbon species under diffuse and dense cloud conditions by UV irradiation were performed. The results indicate that such molecules will be efficiently dehydrogenated in interstellar space. It is argued that the presence of hydrogen in the aliphatic grain material in diffuse clouds results from an equilibrium between dehydrogenation by UV processing and re-hydrogenation by the impinging atomic gas. In dense clouds, the presence of the ice layer will prevent the re-hydrogenation process, causing the carbonaceous grain material to be gradually de-hydrogenated if UV photons are able to penetrate into the dense medium. The implications of this study for the evolution of the carbonaceous component of dust in the interstellar medium are discussed.

**Key words.** ISM: dust, extinction – infrared: ISM: lines and bands – methods: laboratory

## 1. Introduction

Interstellar dust is a ubiquitous component of the Galactic Interstellar Medium (ISM). It is thought to be produced in stellar outflows (Chiar et al. 1998; Nuth 1996). Furthermore, organic solid matter can be produced in the ISM itself by the transformation of condensed ices to refractory organic material upon ultraviolet or ion irradiation (Greenberg 1978; Greenberg et al. 1995; Moore & Donn 1982). The former source gives either silicate or carbonaceous grains depending on whether the outflow originates in an oxygen- or carbon-rich stellar object. This gives rise to separate populations of silicate and carbon dust in the ISM (Mathis et al. 1977; Adamson et al. 1999). The material originating in the ISM itself forms an organic mantle on top of a pre-existing silicate core (Li & Greenberg 1997; Kissel & Krueger 1987).

The composition of the carbonaceous dust in various galactic regions has mainly been probed from the 3.4 $\mu$m band due to the aliphatic C–H stretching mode. Observations show that, relative to the 9.7 $\mu$m silicate feature, the 3.4 $\mu$m band is reduced in the spectra of dense cloud dust as compared to that of diffuse medium dust (Allamandola et al. 1992, 1993; Brooke et al. 1996; Chiar et al. 1996). This difference led to the suggestion that carbonaceous dust material is destroyed inside dense clouds (Pendleton 1999). In view of the continuous cycling of material between the dense and diffuse phases of the interstellar medium (Greenberg 1985; McKee 1989), this would imply that there must be a highly efficient mechanism to form organic species in the ISM to counterbalance the destruction.

To investigate how the cycling of the dust from the dense to the diffuse medium would affect the chemical evolution of the carbonaceous dust material, this article reports on laboratory experiments involving UV processing of simple hydrocarbon species under simulated dense and diffuse cloud conditions. Observations of interstellar dust suggest that the 3.4 $\mu$m band is due to short aliphatic chains attached to aromatic structures (Sandford et al. 1991; Pendleton et al. 1994). Hexane ($C_6H_{14}$) was adopted as it fulfils the $-CH_2-/-CH_3$ ratio of 2–2.5 suggested by the observations (Furton et al. 1999). Ethane ($C_2H_6$) was used to investigate the effect of the chain length on the photodestruction rate. Ethylbenzene ($C_6H_5$–$C_2H_5$) was used to study the case of an aliphatic chain attached to an aromatic structure. Since the carbonaceous dust material is probably characterized by polyaromatic structures

*Send offprint requests to*: G. M. Muñoz Caro,
e-mail: munoz@strw.leidenuniv.nl

(Furton et al. 1999; Mennella et al. 1998; Schnaiter et al. 1999), ethylbenzene is not a fully adequate analog material. However, this study focuses on the aliphatic component of the interstellar organics, and is therefore only concerned with the influence of an attached aromatic ring structure on the destruction efficiency of the aliphatic chain.

In the next paper of this series (Mennella et al. 2001; henceforth Paper II) amorphous carbon grains are the material submitted to photoprocessing, which should be more representative of the carbonaceous matter of interstellar grains. Nevertheless, we wanted to study the processing of a number of well defined species to investigate the dependence on such parameters as the molecular size, the presence of aromatic structures and the thickness of the sample. These results will be used in Paper II to assess the robustness of the results for the more realistic but chemically more complex analog material.

The layout of this paper is as follows: in Sect. 2 of this paper we derive upper limits for the strength of the 3.4 $\mu$m feature of the dense medium and compare these to the 3.4 $\mu$m feature which is observed in the diffuse medium. The experimental protocol is described in Sect. 3. The experimental results are presented in Sect. 4, and discussed in Sect. 5. Section 6 reviews the astrophysical implications. Finally, our conclusions are reported in Sect. 7.

## 2. Quantification of the 3.4 $\mu$m feature in dense clouds

While the reduction of the strength of the interstellar 3.4 $\mu$m feature in dense interstellar regions was already noted by Allamandola et al. (1993), no upper limits have yet been derived quantitatively. Such upper limits are of major importance as a criterion to test any model proposed for this reduction.

A direct integration of the optical depth of the 3.4 $\mu$m band towards embedded protostars is difficult, due to the presence of broad absorption features in this region, such as the 3.05 $\mu$m $H_2O$ band, the "diamond" feature at 3.47 $\mu$m (Allamandola et al. 1992; Chiar et al. 1996; Brooke et al. 1999), the 3.25 $\mu$m band with frozen PAHs as possible carrier (Sellgren et al. 1994, 1995), the CH stretch modes of solid $CH_3OH$ at 3.48 $\mu$m and 3.54 $\mu$m (Grim et al. 1991; Allamandola et al. 1992; Schutte et al. 1996; d'Hendecourt et al. 1996; Dartois et al. 1999) and the "long wavelength shoulder" of the 3.05 $\mu$m feature centered around 3.4 $\mu$m (Willner et al. 1982; Smith et al. 1988). Instead, we obtained upper limits of the 3.4 $\mu$m feature in the dense medium by sequential addition of the 3.4 $\mu$m feature as observed towards a diffuse interstellar medium source, GC IRS6E (adopted from Pendleton et al. 1994), to the spectra of four YSOs, namely GL 2136, MonR2/IRS2, W33A (Brooke et al. 1999), NGC 7538/IRS9 (Allamandola et al. 1992), as well as the background field star Elias 16 (Chiar et al. 1996). This approach can be elucidated in the following way. If a 3.4 $\mu$m feature is present in the absorption spectrum towards a source obscured by dense cloud material, the spectrum is given by

$$F(\nu) = F_{\rm c}(\nu) \cdot {\rm e}^{-\tau_{\rm o}(\nu)} \cdot {\rm e}^{-\tau_{\rm CH}(\nu)} \quad (1)$$

or

$$\ln F(\nu) = \ln F_{\rm c}(\nu) - \tau_{\rm o}(\nu) - \tau_{\rm CH}(\nu) \quad (2)$$

where ln $F$ gives the natural logarithm of the flux $F$, the subscript c denotes "continuum", $\tau_{\rm CH}(\nu)$ describes the 3.4 $\mu$m feature in the dense cloud source, and $\tau_{\rm o}(\nu)$ describes the sum of other absorptions in the relevant spectral region.

After addition of the 3.4 $\mu$m feature as observed in the diffuse interstellar medium, multiplied by a variable factor $C$, to the observed spectrum $\ln F(\nu)$ this becomes

$$\begin{aligned} \ln F(\nu) + C \cdot \tau'_{\rm CH}(\nu) \;=\; & \ln F_{\rm c}(\nu) - \tau_{\rm o}(\nu) - \tau_{\rm CH}(\nu) \\ & + C \cdot \tau'_{\rm CH}(\nu) \end{aligned} \quad (3)$$

where $\tau'_{\rm CH}(\nu)$ gives the 3.4 $\mu$m feature as observed towards the selected diffuse medium source, i.e., GC IRS 6E. Assuming that the profile of any 3.4 $\mu$m feature of dust in dense interstellar clouds is closely comparable to that of dust in the diffuse interstellar medium, it is clear that by choosing $C$ correctly, any 3.4 $\mu$m feature could be eliminated from the spectrum. Elimination of this feature should result in an increase of the "smoothness" of the spectral curve. However, choosing $C$ too large results in overcompensation, and the introduction of structures in the spectrum. Thus by monitoring the maximum value, $C_{\rm max}$, above which the smoothness of the modified spectral curve decreases, a strict upper limit to the strength of the 3.4 $\mu$m band is obtained. The procedure is illustrated in Fig. 1 for GL 2136, NGC 7538/IRS9 and W33A. The upper limits to the 3.4 $\mu$m strength for these objects, which correspond to the values of $C_{\rm max}$ indicated in Fig. 1, are listed in Table 1. Generally, the best constraint for the 3.4 $\mu$m feature is derived from the relatively sharp substructures corresponding to the separation of the $-CH_3$ and $-CH_2-$ asymmetric stretching modes at 3.39 $\mu$m and the separation of the $-CH_2-$ asymmetric and the $-CH_3/-CH_2-$ symmetric stretching mode at 3.46 $\mu$m. Our method shows that the non-observation of these structures in the dense cloud spectra poses strict constraints to the amount of aliphatics that could be present.

In order to compare the composition of the dust particles in the dense and the diffuse medium, Table 1 lists the ratios of the intensity of the 3.4 $\mu$m feature over the 9.7 $\mu$m silicate feature depth. The 9.7 $\mu$m optical depth towards the YSOs, corrected for the underlying emission feature, was calculated using

$$\tau(9.7\ \mu{\rm m}) \approx 1.4 \cdot \tau'(9.7\ \mu{\rm m}) + 1.6 \quad (4)$$

(Willner et al. 1982), where $\tau'(9.7\ \mu{\rm m})$ is the observed depth of the silicate band.

From the values of $\tau_{\rm int}(3.4)/\tau(9.7)$ listed in Table 1, it can be concluded that $\geq$55% of the 3.4 $\mu$m carrier is

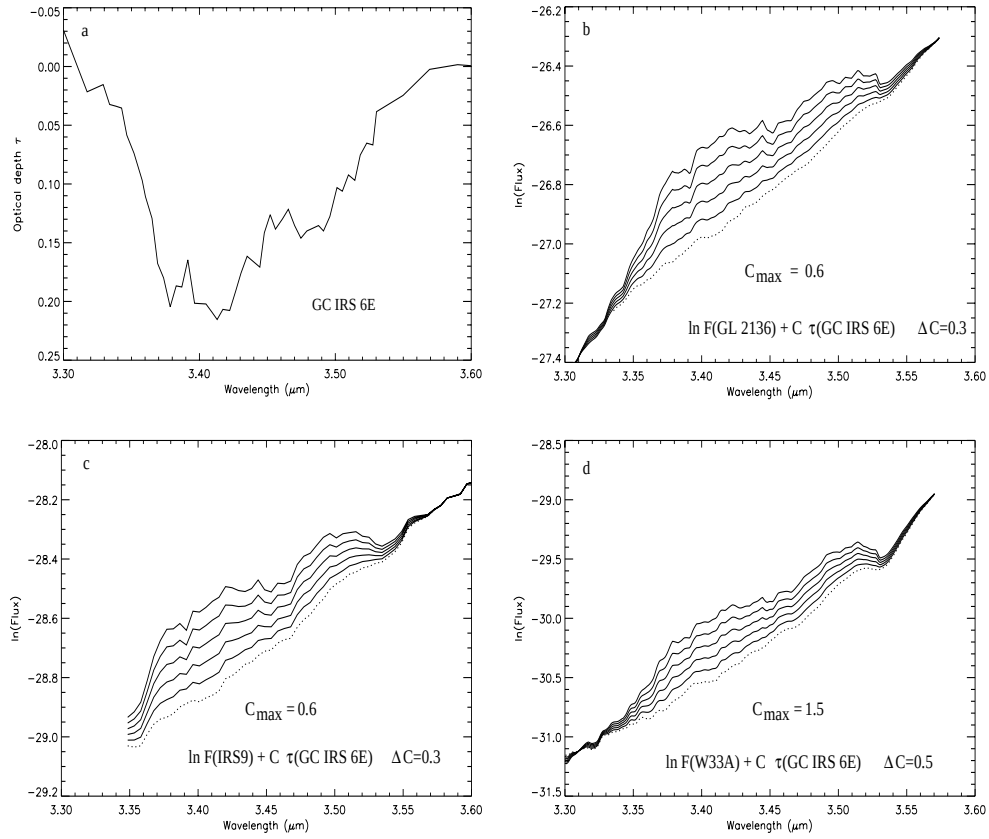


**Fig. 1.** Sequential addition of the 3.4 $\mu$m band of GC IRS 6E (**a**); Pendleton et al. 1994) to the spectra of the embedded Young Stellar Objects (YSOs) GL 2136 (**b**); Brooke et al. 1999), NGC 7538/IRS9 (**c**); Allamandola et al. 1992) and W33A (**d**); Brooke et al. 1999). The spectra of the dense medium probes were smoothed to the same resolution as GC IRS 6E, $\lambda/\Delta(\lambda) \sim 800$. The original spectra are plotted with a dotted line. The different curves on top correspond to addition steps with $\Delta C = 0.3$ for GL 2136 and NGC 7538/IRS9, and $\Delta C = 0.5$ for W33A. The value of $C$ corresponding to the selected upper limit, $C_{\max}$, is indicated

destroyed for GL 2136, $\geq$50% for NGC 7538/IRS9 and $\geq$30% for W33A. For MonR2/IRS2 and Elias 16 the upper limits are less stringent, and could be consistent with no destruction of the 3.4 $\mu$m band. However, the results for GL 2136, NGC 7538/IRS9 and W33A show that, at least towards some embedded sources, the 3.4 $\mu$m feature is substantially reduced.

## 3. Experimental

Details of the experimental set-up have been described earlier (Gerakines et al. 1995). In summary, the set-up consists of a high vacuum chamber ($P \approx 10^{-7}$ mbar) with an IR transparent substrate mounted on a cold finger which is cooled to ~12 K. Samples can be controllably deposited (~$10^{14}$ molec cm$^{-2}$ s$^{-1}$) through a narrow tube. A hydrogen flow discharge lamp provides vacuum UV photons (~5 $10^{14}$ photons cm$^{-2}$ s$^{-1}$; $E_{\rm photon} \geq 6$ eV). The evolution of the sample is monitored by infrared transmission spectroscopy.

The carbonaceous component of interstellar grains was simulated by deposition of a thin layer (typically 0.01 $\mu$m or $N$(C) ~ 3 $10^{16}$ cm$^{-2}$) of various aliphatic and aromatic compounds. Aliphatics were deposited on a CsI substrate window, while ethylbenzene was deposited both on the CsI and a quartz substrate window. The reason for this was that quartz does not adsorb molecules as readily as CsI, thus providing a cleaner substrate and smooth background in the important CH stretching region. This is especially important for experiments using aromatic

**Table 1.** Upper limits for the 3.4 $\mu$m band for various probes of the dense and diffuse medium

| Source | Type | $\tau_{\rm int}(3.4)$ | $\tau(9.7)$ | $\frac{\tau_{\rm int}(3.4)}{\tau(9.7)}$ |
|---|---|---|---|---|
| GL 2136 | YSO, dense | $\leq$0.13 | 5.07[b] | $\leq$0.026 |
| NGC 7538/IRS9 | YSO, dense | $\leq$0.13 | 4.46[b] | $\leq$0.029 |
| MonR2/IRS2 | YSO, dense | $\leq$0.13 | 1[c] | $\leq$0.13 |
| W33A | YSO, dense | $\leq$0.32 | 7.84[b] | $\leq$0.041 |
| Elias 16 | field, dense | $\leq$0.08 | 0.81[e] | $\leq$0.099 |
| GC IRS 6E | field, diffuse | 0.21[a] | 3.6$\pm$0.4[d] | 0.058 |

[a] Pendleton et al. (1994).
[b] Willner et al. (1982).
[c] Beckwith et al. (1976).
[d] Roche & Aitken (1984).
[e] Bowey et al. (1998).

**Table 2.** Band strengths of molecules

| Species | Feature | Position $\mu$m | Position cm$^{-1}$ | $A$ cm mol$^{-1}$ | Ref. |
|---|---|---|---|---|---|
| $H_2O$ | OH stretch | 3.05 | 3279 | 2.0 $10^{-16}$ | *a* |
| $C_2H_6$ | CH stretch | 3.4 | 2940 | 1.0 $10^{-17}$ | *b* |
| $C_6H_{14}$ | CH stretch | 3.4 | 2940 | 3.5 $10^{-17}$ | *b* |
| Ethylb. | aliph. CH st. | 3.4 | 2940 | 1.7 $10^{-17}$ | *c* |

[a] Hagen et al. (1981).
[b] Wexler (1967).
[c] Obtained from strength relative to the aromatic feature.

species, which have relatively weak C–H stretching bands. For quartz substrates the infrared range is limited to 4000–2200 cm$^{-1}$. The species used were hexane ($C_6H_{12}$, Merck, ≥97%), ethane ($C_2H_6$, Praxair, 99.99%) and ethylbenzene ($C_6H_5$–$C_2H_5$, Merck-Schuchardt, >99%). A layer thickness of 0.01 $\mu$m corresponds to typical dimensions of the carbonaceous component of interstellar dust (Mathis et al. 1977; Li & Greenberg 1997). To emulate the icy mantle accreting in dense clouds, the carbonaceous layer was covered by an $H_2O$ ice cap, triply distilled, of typically ∼0.01 $\mu$m ($N(H_2O) = 3\ 10^{16}$ cm$^{-2}$). This is consistent with mantle thicknesses expected for grains in dense clouds (Schutte & Greenberg 1991; Kim & Martin 1996). The ice mixture $H_2O$:CO:$NH_3$ = 5:2:1 (CO, Praxair, 99.997%; $NH_3$, Praxair, 99.9995%) was also employed. To reproduce diffuse medium conditions, the hydrocarbon layer was sandwiched in argon (Praxair, 99.9997%), layer thickness ∼0.5 $\mu$m, to isolate it from the background gas in the vacuum set-up (mostly $H_2O$; Gerakines et al. 1996). Both the diffuse and dense medium analog samples were exposed to UV radiation, with infrared spectra taken at regular intervals. Experimental parameters are listed in Table 3. The carbon column density of the sample, $N$(C), and the column density of the ice cap on top of the carbon layer, $N$(ice), were obtained by integration of the spectral features:

$$N = \frac{\int \tau \mathrm{d}\nu}{A} \tag{5}$$

where $N$ is the column density in cm$^{-2}$, $\tau$ the optical depth of the band, and $A$ the band strength (Table 2).

## 4. Results

Figure 2 shows a spectroscopic record of the photochemical evolution of a dense medium analog sample consisting of a hexane layer covered by water ice (Exp. No. 2, Table 3). The spectrum shows that, as a result of the photolysis, the CH stretching mode at 2940 cm$^{-1}$ (3.4 $\mu$m) and the CH bending modes around 1400 cm$^{-1}$ (7.1 $\mu$m) are strongly reduced. Although features due to CO and $CO_2$ develop during irradiation, it was found by means of control experiments, where only water was deposited and irradiated, that accretion and photolysis of background

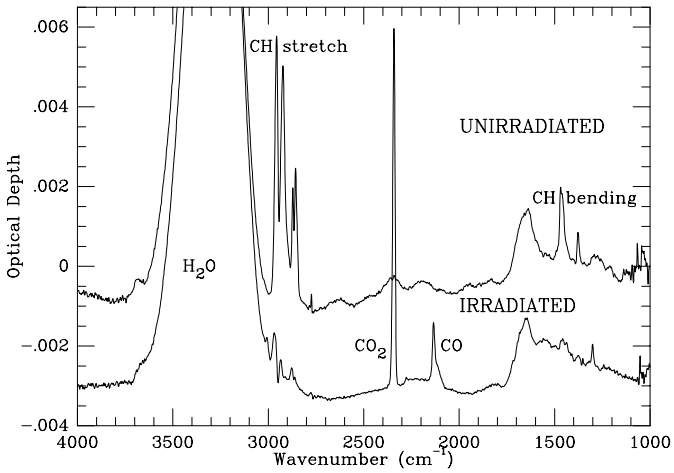


**Fig. 2.** Infrared spectrum of a layer of hexane covered by $H_2O$ ice, corresponding to Exp. No. 2 in Table 3, before and after irradiation. For clarity, the spectra have been offset

gases, i.e. contamination, can fully account for the formation of these features.

Figure 3 traces the evolution of the 3.4 $\mu$m feature as a function of irradiation dose for three samples with similar thickness of the hexane layer but with varying ice thickness (see Table 3). Error bars were obtained by performing the integration of the feature with polynomial baselines of different order. It shows that the destruction of the CH bond decreases somewhat for thicker ice caps, apparently due to absorption of the UV by the ice. Figure 4 compares the destruction of the 3.4 $\mu$m feature for samples with different hexane thickness but similar ice cap. Clearly, the destruction rate of the 3.4 $\mu$m feature is higher for thinner carbon layers. No significant difference was found between the destruction of the 3.4 $\mu$m feature of ethane and hexane, indicating that the length of the aliphatic chain is not relevant (Fig. 5). Furthermore, the composition of the ice cap, whether pure $H_2O$ or $H_2O$:CO:$NH_3$ = 5:2:1, does not appreciably affect the evolution of the 3.4 $\mu$m band under photolysis.

To quantify these results, we calculated the destruction cross section $\sigma_{\mathrm{des}}$ for aliphatic CH bonds using

$$\frac{\mathrm{d}\tau_{\mathrm{int}}(\mathrm{CHstretch})}{\mathrm{d}t} = -\Phi(\mathrm{UV}).\sigma_{\mathrm{des}}.\tau_{\mathrm{int}}(\mathrm{CHstretch}) \tag{6}$$

where $\tau_{\mathrm{int}}$(CHstretch) equals the integrated optical depth and $\Phi$(UV) is the flux of the lamp at the position of the sample. Note that Eq. (6) does not take into account the attenuation of the UV flux by the ice cap. Therefore $\sigma_{\mathrm{des}}$ as obtained from this equation should generally be regarded as a convenient working parameter that allows an estimate of the destruction of the 3.4 $\mu$m band under equivalent interstellar circumstances, rather than a "true" molecular destruction cross section. Table 3 lists $\sigma_{\mathrm{des}}$ measured upon initial irradiation. The destruction cross section decreases typically by a factor ∼10 after 3 hr irradiation (∼5 $10^{18}$ photon cm$^{-2}$). This may be caused by chemical changes induced by the processing, e.g. the formation of

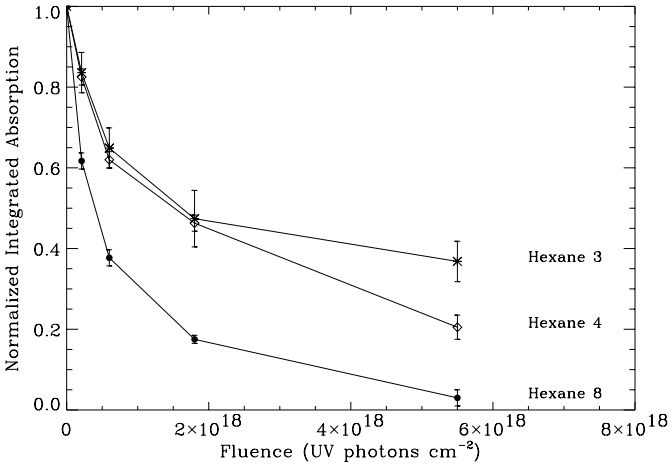


**Fig. 3.** Destruction of the 3.4 $\mu$m feature for experiments with similar thickness of the hexane layer. Numbers refer to entries in Table 3. Hexane 3 corresponds to a $H_2O$ ice cap of 5.3 $10^{16}$ molec cm$^{-2}$, Hexane 4 to a cap of 2.9 $10^{15}$ molec cm$^{-2}$, and Hexane 8 to a hexane sample sandwiched between two argon layers

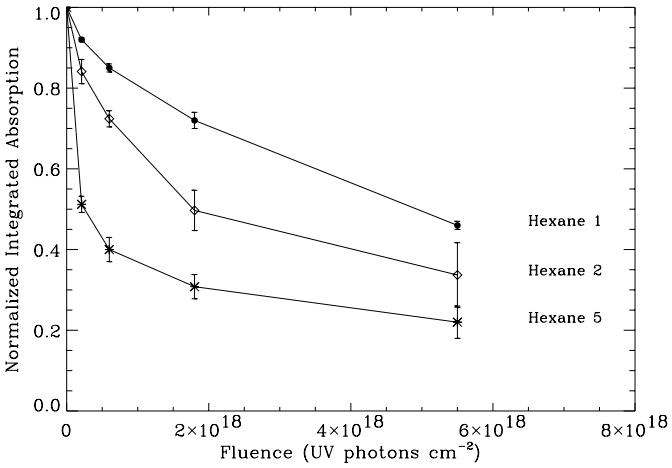


**Fig. 4.** Destruction of the 3.4 $\mu$m feature for experiments with similar thickness of the ice cap and different hexane thicknesses. Numbers refer to entries in Table 3. Hexane 1 corresponds to a layer of 3.4 $10^{17}$ C atoms cm$^{-2}$, Hexane 2 to 7.1 $10^{16}$ C atoms cm$^{-2}$, and Hexane 5 to 3.5 $10^{16}$ C atoms cm$^{-2}$

unsaturated and/or ring structures, or by the reduction on the number of available CH bonds.

Figure 6 shows the destruction of the 3.4 $\mu$m feature of ethylbenzene capped by water ice as function of the irradiation dose (Exp. No. 10, Table 3). Note that the applied irradiation dose is higher than it was for the pure hydrocarbons (cf., Figs. 3 and 4). Even though the destruction of the aliphatic 3.4 $\mu$m band of ethylbenzene is less rapid than for pure aliphatic molecules such as hexane, still 40% is destroyed after 3 hr of irradiation (5 $10^{18}$ photons cm$^{-2}$) and 80% after 15 hr (2.5 $10^{19}$ photons cm$^{-2}$). The difference might be due to the presence of the aromatic ring giving more stability to the molecule by allowing distribution of the UV induced excitation.

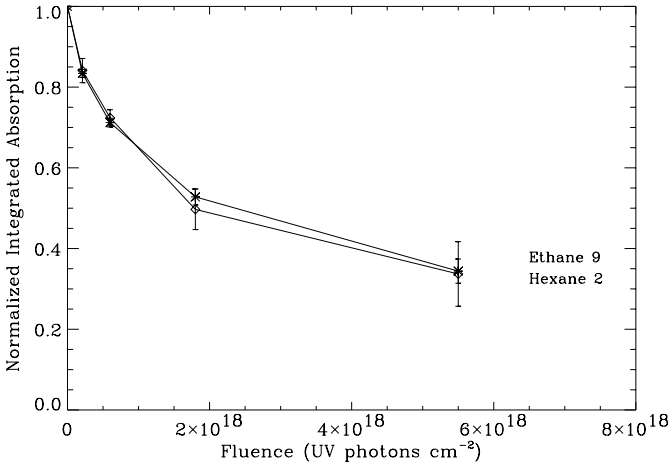


**Fig. 5.** Destruction of the 3.4 $\mu$m feature for a hexane and an ethane sample. Numbers refer to entries in Table 3

**Table 3.** Experimental parameters

| Exp. No. | Species | $N$(C) cm$^{-2}$ | $N$(ice[a]) cm$^{-2}$ | $\sigma_{\rm des}$(initial) cm$^2$ |
|---|---|---|---|---|
| 1 | Hexane | 3.4 $10^{17}$ | 2.3 $10^{16}$ | 3.6 $10^{-19}$ |
| 2 | Hexane | 7.1 $10^{16}$ | 2.8 $10^{16}$ | 8.4 $10^{-19}$ |
| 3 | Hexane | 6.8 $10^{16}$ | 5.3 $10^{16}$ | 8.6 $10^{-19}$ |
| 4 | Hexane | 6.5 $10^{16}$ | 2.9 $10^{15}$ | 9.0 $10^{-19}$ |
| 5 | Hexane | 3.5 $10^{16}$ | 3.1 $10^{16}$ | 3.2 $10^{-18}$ |
| 6 | Hexane | 2.4 $10^{16}$ | 3.7 $10^{16}$ | 2.6 $10^{-18}$ |
| 7 | Hexane | 9.5 $10^{16}$ | 3.8 $10^{16}$[b] | 6.4 $10^{-19}$ |
| 8 | Hexane | 6.1 $10^{16}$ | -[c] | 2.2 $10^{-18}$ |
| 9 | Ethane | 1.4 $10^{17}$ | 3.1 $10^{16}$ | 8.2 $10^{-19}$ |
| 10 | Ethylb. | 3.8 $10^{16}$ | 7.1 $10^{16}$ | 5.0 $10^{-19}$ |

[a] $H_2O$ ice, unless otherwise noted.
[b] Ice mixture $H_2O$:CO:$NH_3$ = 5:2:1.
[c] Sandwiched in Ar.

## 5. Discussion

The decrease of the 3.4 $\mu$m band of the carbon-based materials upon irradiation may result from a number of mechanisms. First, the material may be destroyed by highly oxidizing species formed by photolysis of the ice cap, such as OH radicals. Second, reactions with ice photofragments may insert oxygen containing groups like hydroxy and carbonyl into the carbon skeleton. Such groups strongly decrease the intensity of nearby CH stretching modes (Wexler 1967). Finally, because the UV photon energy is larger than the bond enthalpy (∼4.3 eV for aliphatic CH bonds), photolysis may break CH bonds and dehydrogenate the carbonaceous sample.

The experimental results suggest that dehydrogenation is the main cause of the decrease of the CH stretching mode. First, it is clear that destruction is higher with thinner ice caps (Table 3), arguing against any mechanism in which the interaction with water ice

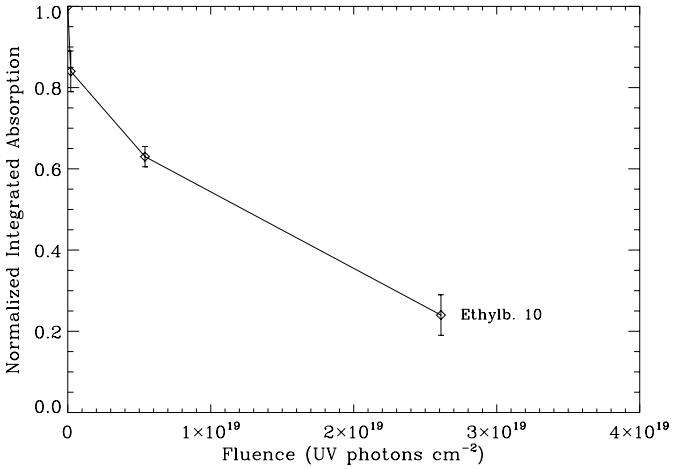


**Fig. 6.** Destruction of the 3.4 $\mu$m feature of ethylbenzene (Table 3, Exp. 10)

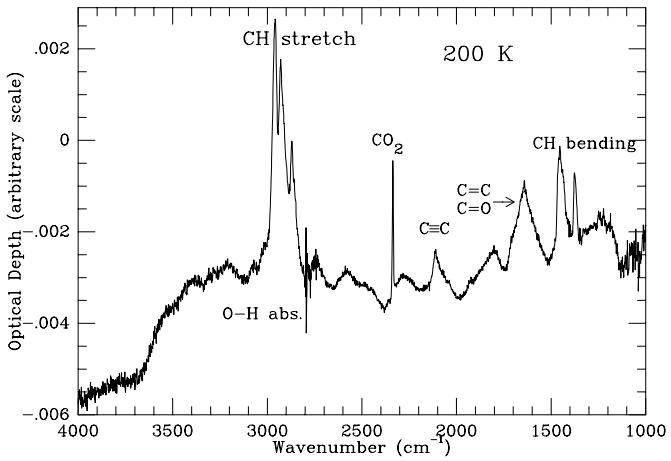


**Fig. 7.** Residue spectrum of a layer of hexane covered by $H_2O$ ice after 3 hr of UV-irradiation (5 $10^{18}$ photon cm$^{-2}$) and warm-up to 200 K to evaporate the ice cap

photoproducts causes the reduction. Indeed, the highest destruction is obtained when the hydrocarbon layer is covered only with argon. Second, if the carbonaceous layer is broken up by the attack of, say, OH radicals, the growth of features of new species, e.g. CO, $CO_2$, HCO, should be observed. Although some CO and $CO_2$ is formed during the photolysis (Fig. 2), comparison with blank experiments shows this can be explained by accretion and photolysis of background gases, indicating that breakdown of the carbon skeleton accounts for less than ∼2% of the decrease of the 3.4 $\mu$m band. Third, the spectrum of the residue, obtained from Experiment 1 (Table 3) after 3 hours of irradiation (∼5 $10^{18}$ photon cm$^{-2}$) of a hexane/ice sample and subsequent warm-up to 200 K, shows little evidence of oxygen containing groups (Fig. 7). Perhaps the broad band underlying the CH stretching mode centered at ∼3300 cm$^{-1}$ could derive from the OH stretch of hydroxy (–OH) groups, although another possibility is the presence of some residual $H_2O$ locked inside the residue (this possibility is supported by the trapping of some $CO_2$ in the residue). Furthermore, while the position of the feature at 1645 cm$^{-1}$ is indicative of unsaturated C=C bonds, a weak shoulder at ∼1700 cm$^{-1}$ may indicate the presence of carbonyl (C=O) groups in the residue. The weakness of these bands shows that less than 20% of the C atoms are bound to O-containing groups, too little to explain the reduction of the CH stretching mode. Finally, the strong features in the residue spectrum of unsaturated C–C bonds constitute direct evidence for the importance of dehydrogenation. The residue spectra of ice capped irradiated ethylbenzene (Exp. No. 10) at 200 K shows no significant features. For the C=O stretching mode at ∼1700 cm$^{-1}$ we obtained $N$(C=O)/$N$(CH) < 0.1, where $N$(CH) refers to the column density obtained from integration of the CH stretch after deposition. For the –OH deformation mode at ∼1350 cm$^{-1}$ it was found $N$(OH)/$N$(CH) < 0.1. We thus conclude that dehydrogenation by interaction with UV photons is responsible for the decrease of the CH stretching features in our experiments.

## 6. Astrophysical implications

Our experimental results show that hydrocarbon molecules will be dehydrogenated in the diffuse medium. We derive that for aliphatic chains, like hexane, dehydrogenation by ∼80% requires a dose of 5 $10^{18}$ UV photon cm$^{-2}$ (Fig. 4). With a UV field 8 $10^7$ photon cm$^{-2}$ s$^{-1}$ ($E_{\rm ph} \geq 6$ eV) in the diffuse galactic medium (Mathis et al. 1983), this corresponds to 2 $10^3$ yr. The aliphatic component of ethylbenzene requires a ≈5 times higher dose to achieve an 80% dehydrogenation (Fig. 6), corresponding to ≈1 $10^4$ yr. In Paper II it will be reported that the dehydrogenation of more complex carbonaceous materials, which are likely more analogous to interstellar dust, also proceeds efficiently.

Our results suggest that aliphatic solids can only survive in the diffuse interstellar medium if a hydrogenation mechanism is active (Mennella et al. 1999). Such a mechanism was earlier proposed to explain the "turn-on" of the 3.4 $\mu$m feature in proto-planetary nebula (Schnaiter et al. 1999). A bountiful stock of atomic hydrogen is present in the gas phase in the diffuse ISM. If the loss of hydrogen is balanced by the formation of aliphatic groups between solid carbon and gaseous hydrogen, the following applies:

$$F(\mathrm{H}) \cdot \sigma_{\rm grain} \cdot f \;=\; F_{\rm DiM}(\mathrm{UV}) \cdot \sigma_{\rm des}(\mathrm{CH}) \cdot n_{\rm grain}(\mathrm{CH}) \quad (7)$$

where $\sigma_{\rm grain}$ is the grain cross section, $F$(H) the flux of atomic hydrogen, $F_{\rm DiM}$(UV) the UV flux in the diffuse medium, $n_{\rm grain}$(CH) the number of aliphatic CH bonds in the grain/grain mantle, and $f$ is the fraction of the impinging hydrogen atoms that bonds with the carbonaceous material ($0 \leq f \leq 1$). To quantify Eq. (7), we note

$$\left[\frac{n_{\rm grain}(\mathrm{CH})}{\sigma_{\rm grain}}\right] = \left[\frac{\sigma_{\rm grain}}{n(\mathrm{H})}\right]^{-1} \cdot \left[\frac{n_{\rm grain}(\mathrm{C})}{n(\mathrm{H})}\right] \cdot \left[\frac{n_{\rm grain}(\mathrm{CH})}{n_{\rm grain}(\mathrm{C})}\right] \cdot (8)$$

The latter three quantities refer to properties of carbonaceous grains/grain mantles in the diffuse ISM, i.e. the grain surface area per H atom, the number of carbon

atoms in grains per H atom, and the average number of aliphatic CH bonds per C atom within grains, respectively.

$F$(H) is obtained from:

$$F(\mathrm{H}) = n(\mathrm{H}) \cdot \sqrt{\frac{8kT}{\pi m}}. \quad (9)$$

For the hydrogen density we adopt $n(\mathrm{H}) = 4$ cm$^{-3}$, the average density along the line of sight towards Cyg. OB2 #12, the prototypical source for studying the 3.4 $\mu$m feature of the local diffuse medium (Whittet et al. 1997). Furthermore, $T = 100$ K, $F_{\mathrm{DiM}}(\mathrm{UV}) = 8\ 10^7$ UV photons cm$^{-2}$ s$^{-1}$, $E_{\mathrm{ph}} \geq 6$ eV (Mathis et al. 1983), $\left[\frac{n(\mathrm{H})}{\sigma_{\mathrm{grain}}}\right] = 2.5\ 10^{19}$ cm$^{-2}$ (Li & Greenberg 1997; Mathis 1996), $\left[\frac{n_{\mathrm{grain}}(\mathrm{C})}{n(\mathrm{H})}\right] = 1.5\ 10^{-4}$ (Li & Greenberg 1997; Mathis 1996), $\left[\frac{n_{\mathrm{grain}}(\mathrm{CH})}{n_{\mathrm{grain}}(\mathrm{C})}\right] = 0.13$ (Schutte et al. 1998). We adopt $\sigma_{\mathrm{des}}(\mathrm{CH}) \approx 5\ 10^{-19}$ cm$^2$, as obtained for ethylbenzene (Sect. 4.2). Equations (5–7) then yield $f = 3.4\ 10^{-2}$, i.e., ∼3% of the impinging H atoms are required to bond to the carbonaceous matter to balance the photo-dehydrogenation. This is well within the limits found by experiments involving bombardment by atomic hydrogen of carbon grains ($f \approx 6\ 10^{-2}$; Mennella et al. 1999). With the lower destruction cross sections for CH bonds obtained for the more realistic analog material in Paper II, rehydrogenation should dominate dehydrogenation even more.

Inside dense clouds grains will be covered by an ice cap, consisting primarily of $H_2O$ with in addition CO, $CO_2$, probably $NH_3$, etc. (Gibb et al. 2000; and references therein). This cap has a thickness of ∼0.01 $\mu$m, i.e., ∼30 molecular layers (Schutte & Greenberg 1991). It seems unlikely that any atomic hydrogen would be able to penetrate the ice mantle and reach the carbonaceous material. First, hydrogen atoms can be immobilized in ice at ∼12 K, for example, in Ar (van Ijzendoorn et al. 1983). Second, in the presence of frozen CO, a ubiquitous component of interstellar ice, formation of HCO could scavenge diffusing H atoms (van Ijzendoorn et al. 1983). Third, atomic hydrogen is scarce in the dense cloud environment, since most of the hydrogen will be in the form of $H_2$. It therefore seems likely that hydrogenation of carbonaceous grain material will cease inside dense clouds. However, in spite of the ice cover, our experiments show that dehydrogenation of the carbonaceous material will proceed as long as some UV is present (Sect. 4). Therefore the carbonaceous grain material inside dense clouds will be dehydrogenated gradually.

The results in Sect. 4 indicate that the UV fluence necessary to achieve 80% dehydrogenation (the reduction consistent with the observational constraints; Sect. 2) equals ∼2.5 $10^{19}$ photons cm$^{-2}$ (Fig. 6). Very similar requirements for the amount of processing will be reported in Paper II, based on experiments with the more realistic analog material. The internal UV field cannot provide such a processing in dense clouds. Thus, the penetration of the galactic radiation field, involving intense short term exposures of grains during a fraction of the lifetime of an interstellar cloud when they reside in the outer regions, should be the driving factor for the reduction of the 3.4 $\mu$m feature (see an extended discussion in Paper II). Whether this scenario is realistic depends on the nature of the circulation of matter in dense clouds. Theoretical modelling of this effect as well as of the penetration of radiation into filamentary clouds is required to better understand the extent to which grains in dense regions may be UV-processed.

It is intriguing that the dose estimated from the reduction of the 3.4 $\mu$m feature is very similar to the dose required to produce the amount of $CO_2$ ice which is observed in Taurus towards the field star Elias 16 (3 $10^{19}$ photons cm$^{-2}$; Whittet et al. 1998). Thus, the present results may point to the importance of UV processing for the chemical evolution of dense cloud ices.

In this scenario, the observed decrease of the CH stretching mode under dense cloud conditions can be achieved without destroying the carbonaceous grain material. This alleviates the requirement of highly efficient formation of carbonaceous matter in the ISM.

The astrophysical implications of our results are independent of the exact morphology of the carbonaceous dust material. They equally apply to all of the grains mentioned in Sect. 1, i.e., the physically separate populations of silicate and carbon grains, and the silicate core/carbonaceous mantle particles.

*Acknowledgements.* We thank T. Y. Brooke and J. E. Chiar for kindly providing us with their observational data files. One of us, G.M.M.C., thanks the Max-Planck-Institut für Aeronomie at Katlenburg-Lindau, in particular the COSAC-Rosetta group, for a fellowship. One of us, V. M., has been supported by ASI and MURST research contracts.

## References

Adamson, A. J., Whittet, D. C. B., Chrysostomou, A., et al. 1999, ApJ, 512, 224
Allamandola, L. J., Sandford, S. A., Tielens, A. G. G. M., & Herbst, T. M. 1992, ApJ, 399, 134
Allamandola, L. J., Sandford, S. A., Tielens, A. G. G. M., & Herbst, T. M. 1993, Science, 260, 64
Beckwith, S., Evans II, N. J., Becklin, E. E., & Neugebauer, G. 1976, ApJ, 208, pt. 1, 390
Bowey, J. E., Adamson, A. J., & Whittet, D. C. B. 1998, MNRAS, 298, 131
Brooke, T. Y., Sellgren, K., & Smith, R. G. 1996, ApJ, 459, 209
Brooke, T. Y., Sellgren, K., & Geballe, T. R. 1999, ApJ, 517, 883
Chiar, J. E., Adamson, A. J., & Whittet, D. C. B. 1996, ApJ, 472, 665
Chiar, J. E., Pendleton, Y. J., Geballe, T. R., & Tielens, A. G. G. M. 1998, ApJ, 507, 281
Dartois, E., Schutte, W. A., Geballe, T. R., et al. 1999, A&A, 342, 32
d'Hendecourt, L., Jourdain de Muizon, M., Dartois, E., et al. 1996, A&A, 315, 365
Furton, D. G., Laiho, J. W., & Witt, A. N. 1999, ApJ, 526, 752

Gerakines, P. A., Schutte, W. A., Greenberg, J. M., & van Dishoeck, E. F. 1995, A&A, 296, 810
Gerakines, P. A., Schutte, W. A., & Ehrenfreund, P. 1996, A&A, 312, 289
Gibb, E. L., Whittet, D. C. B., Schutte, W. A., et al. 2000, ApJ, 536, 347
Greenberg, J. M. 1985, in Light on Dark Matter, ed. F. Israel (Dordrecht: Reidel), 177
Greenberg, J. M. 1978, in Cosmic Dust, ed. J. A. M. McDonnell (Wiley), 187
Greenberg, J. M., Li, A., Mendoza Gómez, C. X., et al. 1995, ApJ, 455, L177
Grim, R. J. A., Baas, F., Greenberg, J. M., Geballe, T. R., & Schutte, W. A. 1991, A&A, 243, 473
Hagen, W., Tielens, A. G. G. M., & Greenberg, J. M. 1981, Chem. Phys., 56, 367
Kim, S.-H., & Martin, P. G. 1996, ApJ, 462, 296
Kissel, J., & Krueger, F. R. 1987, Nature, 326, 755
Li, A., & Greenberg, J. M. 1997, A&A, 323, 566
Mathis, J. S., Rumpl, W., & Nordsieck, K. H. 1977, ApJ, 217, 425
Mathis, J. S., Mezger, P., & Panagia, N. 1983, A&A, 128, 212
Mathis, J. S. 1996, ApJ, 472, 643
McKee, C. F. 1989, in Interstellar Dust, ed. L. J. Allamandola, & A. G. G. M. Tielens (Dordrecht: Kluwer), 431
Mennella, V., Colangeli, L., Bussoleti, E., et al. 1998, ApJ, 507, 177
Mennella, V., Brucato, J. R., Colangeli, L., & Palumbo, P. 1999, ApJ, 524, L71
Mennella, V., Muñoz Caro, G. M., Ruiterkamp, R., et al. 2001, A&A, 367, 355, Paper II
Moore, M. H., & Donn, B. 1982, ApJ, 257, L47
Nuth III, J. A. 1996, in The Cosmic Dust Connection, ed. J. M. Greenberg (Dordrecht: Kluwer), 205
Pendleton, Y. J., Sandford, S. A., Allamandola, L. J., Tielens, A. G. G. M., & Sellgren, K. 1994, ApJ, 437, 683
Pendleton, Y. J. 1999, in Solid Interstellar Matter: The ISO Revolution, ed. L. d'Hendecourt, C. Joblin, & A. Jones (Berlin: Springer), 119
Roche, P. F., & Aitken, D. K. 1984, MNRAS, 208, 481
Sandford, S. A., Allamandola, L. J., Tielens, A. G. G. M., et al. 1991, ApJ, 371, 607
Schnaiter, M., Henning, Th., Mutschke, H., et al. 1999, ApJ, 519, 687
Schutte, W. A., & Greenberg, J. M. 1991, A&A, 244, 190
Schutte, W. A., Gerakines, P. A., Geballe, T. R., van Dishoeck, E. F., & Greenberg, J. M. 1996, A&A, 315, L333
Schutte, W. A., van der Hucht, K. A., Whittet, D. C. B., et al. 1998, A&A, 337, 261
Sellgren, K., Smith, R. G., & Brooke, T. Y. 1994, ApJ, 433, 179
Sellgren, K., Brooke, T. Y., Smith, R. G., & Geballe, T. R. 1995, ApJ, 449, L69
Smith, R. G., Sellgren, K., & Tokunaga, A. T. 1988, ApJ, 334, 209
van Ijzendoorn, L. J., Allamandola, L. J., Baas, F., & Greenberg, J. M. 1983, J. Chem. Phys., 78, 7018
Wexler, A. S. 1967, Appl. Spectrosc. Rev., 1, 29
Whittet, D. C. B., Boogert, A. C. A., Gerakines, P. A., et al. 1997, ApJ, 490, 729
Whittet, D. C. B., Gerakines, P. A., Tielens, A. G. G. M., et al. 1998, ApJ, 498, 159
Willner, S. P., Gillett, F. C., Herter, T. L., et al. 1982, ApJ, 253, 174